

Exploring Tellurides: Synthesis and Characterization of New Binary, Ternary, and Quaternary Compounds

Jing Li^{1,2} and Hong-You Guo

Department of Chemistry, Rutgers University, Camden, New Jersey 08102-1634

and

Davide M. Proserpio¹ and Angelo Sironi

Istituto di Chimica Strutturistica, Università di Milano, 20133 Milan, Italy

Received August 30, 1994; in revised form December 9, 1994; accepted January 4, 1995

A fast-growing interest in solid state telluride chemistry has taken place during the past several years. Our research in this area has been primarily on the development and applications of several synthetic techniques that can be applied to the synthesis of the tellurides over a wide temperature range (100–1200°C). These techniques include chemical vapor transport, molten-salt, and hydro(solvo)thermal methods. In this article, we report five binary, ternary, and quaternary metal tellurides, BaTe₂, TaCu₃Te₄, RbTaCu₂Te₄, K₂BaSnTe₄, and K₂Ag₂SnTe₄, synthesized by the molten-salt (alkali-metal polytelluride flux) reactions at intermediate temperatures (400–550°C). The crystal structures of these compounds have been determined by single crystal X-ray diffraction techniques. Crystal data: BaTe₂, space group *I4/mcm* (No. 140), *a* = 7.181(1), *c* = 8.898(2) Å, *Z* = 4, *R*1 = 1.55%, *wR*2 = 3.46%; RbTaCu₂Te₄, space group *P2₁cn* (No. 33), *a* = 5.982(2), *b* = 20.316(3), *c* = 8.192(2) Å, *Z* = 4, *R*1 = 7.13%, *wR*2 = 4.95%; TaCu₃Te₄, space group *P-43m* (No. 215), *a* = 5.930(2) Å, *Z* = 1, *R*1 = 2.40%, *wR*2 = 6.48%; K₂BaSnTe₄, space group *I-43m* (No. 217), *a* = 8.393(1) Å, *Z* = 2, *R*1 = 2.52%, *wR*2 = 3.56%; K₂Ag₂SnTe₄, space group *I-42m* (No. 121), *a* = 8.732(5), *c* = 7.425(3) Å, *Z* = 2, *R*1 = 3.06%, *wR*2 = 7.25%. © 1995

Academic Press, Inc.

INTRODUCTION

Research in the chemistry and physics of solid state metal tellurides has become very active during the past several years. A variety of synthetic techniques have been applied to the synthesis of these materials, which has led to the discovery of numerous new binary, ternary, and quaternary telluride compounds (1–7). The high-temperature techniques, such as chemical vapor

transport (CVT) reactions (8), remain important in solid state synthesis, and are commonly used in the preparation and crystallization of tellurides (1–3, 5). However, the study of metastable phases has necessitated the use of lower temperature syntheses. Among various methods, the most quickly adopted one is the molten-salt technique (9), often referred to as flux growth technique (10, 11). When applied to the synthesis of solid state tellurides, or chalcogenides in general, the alkali-metal polychalcogenides (A_xQ_y , *A* = alkali metal, *Q* = S, Se, or Te, and in general $y > x$) are used as the salts or fluxes in most of the reactions. They play the key role in controlling the reaction temperatures. These salts (melts) of relatively low melting points become liquified in the temperature range ~200–500°C (11), and at these temperatures they behave much the same as an ordinary solvent. Crystallization of a compound from such a melt is very similar to the crystallization of an organic or organometallic species from a solution at room temperature.

Our recent work on the applications of the flux growth techniques has resulted in a number of tellurides synthesized at intermediate temperatures (400–550°C). Here, we describe the structures and the electronic properties of several telluride compounds prepared from alkali-metal polytelluride melts.

SAMPLE PREPARATION

All alkali-metal (*A*) polytelluride fluxes were prepared by mixing A_2Te and Te in the appropriate ratio. Various A_2Te precursors were obtained by reaction of tellurium powders (99.8%, Strem Chemicals, Inc., Newburyport, MA) in stoichiometric proportion with the metals dissolved in liquid ammonia (12).

BaTe₂ (I). Single crystals of BaTe₂ were obtained from a Na₂Te/BaTe/Te flux at 525°C. Na₂Te and BaTe

¹ To whom correspondence should be addressed.

² Henry Dreyfus Teacher-Scholar 1994–1998.

were used as precursors in this reaction (Na and Ba, 99.7%, Strem Chemicals). Samples of Na₂Te and BaTe were freshly prepared and stored under an inert atmosphere prior to use. In an attempt to synthesize the quaternary barium-containing tellurides, 0.0868 g (0.5 mmole) of Na₂Te, 0.1325 g (0.5 mmole) of BaTe, 0.0905 g (0.5 mmole) of Ta (>99.9%, Aldrich Chemical Co., Inc., Milwaukee, WI) and 0.3828 g (3 mmole) of Te were mixed under an inert atmosphere. The mixture was transferred to a Pyrex tube and sealed under vacuum. The tube was slowly heated to 525°C and was kept at 525°C for 4 days. A slow cooling (4°C/hr) followed and the temperature was reduced from 525 to 150°C. Dimethylformamide (DMF), anhydrous ethyl alcohol, and ethyl ether were then used successively to isolate and dry the products. Black, column-like crystals of BaTe₂ were found. Direct reaction of a stoichiometric mixture of elements at 600°C gave a yield of approximately 80%.

RbTaCu₂Te₄ (II) and TaCu₃Te₄ (III). Both compounds were crystallized in a Rb₂Te/Te flux at 450°C. The black, column-like crystals of RbTaCuTe₄ were isolated from a reaction mixture containing 0.149 g (0.5 mmole) of Rb₂Te (Rb, 99.9+%, Strem Chemicals), 0.090 g (0.5 mmole) of Ta, 0.032 g (0.5 mmole) of Cu (99.5%, Aldrich Chemical Co.), and 0.447 g (3.5 mmole) of Te as starting materials. The reaction was carried out in a sealed Pyrex tube of ca. 6 in. length at 450°C for 4 days. After the heating process, it was then cooled slowly to 120°C (cooling rate: 4°C/hr). The excess flux was removed from the final product with DMF. Black, rhombododecahedral-shaped crystals of TaCu₃Te₄ were also isolated.

K₂BaSnTe₄ (IV). The synthesis of K₂BaSnTe₄ was carried out in a K₂Te/BaTe/Te flux. The heating scheme was the same as previously described for (II) and (III). Black, nearly cubic-shaped crystals of (IV) were grown from a mixture of 0.3087 g (1.5 mmole) of K₂Te (K, 98%, Strem Chemicals), 0.1325 g (0.5 mmole) of BaTe, 0.0594 g (0.5 mmole) of Sn (99.8%, Aldrich Chemical Co.), and 0.3190 g (2.5 mmole) of Te. Elemental analysis by EDS gave an average of K₂BaSnTe_{4.2} for the selected crystals. Powder X-ray analysis on the sample showed a qualitative yield of ~40% K₂BaSnTe₄ along with several impurity phases.

K₂Ag₂SnTe₄ (V). K₂Ag₂SnTe₄ was crystallized in a K₂Te/Te flux. The heating scheme was the same as previously described for (II), (III), and (IV). The reaction of 0.206 g (1.0 mmole) of K₂Te, 0.108 g (1.0 mmole) of Ag, 0.0594 g (0.5 mmole) of Sn, and 0.319 g (2.5 mmole) of Te yielded black, thin column-like crystals of (V). Selected crystals were used in the elemental analysis (EDS), and an average of K_{2.0}Ag_{1.7}Sn_{1.3}Te_{3.9} was obtained for this compound.

STRUCTURE ANALYSIS

The structures of all five compounds were solved by single crystal X-ray diffraction methods. Data collections were carried out on the Enraf-Nonius CAD4 diffractometer employing graphite-monochromated MoK α radiation ($\lambda = 0.71069$ Å). Unit cell constants were obtained from refinement on 25 accurately centered reflections. Data were collected at room temperature with omega scan and theta limits 3–27° for all the samples. Direct methods (13) were employed for the structure solutions. All structures were refined by full-matrix least-squares on F_o^2 with the SHELXL-93 programs (14). Absorption corrections were applied using an empirical Ψ -scan method (15). To improve the refinement an isotropic extinction parameter was refined for BaTe₂ (I), TaCu₃Te₄ (III), and K₂BaSnTe₄ (IV). Absolute configurations have been assigned for the four noncentrosymmetric structures (II)–(V), using Flack absolute structure parameter (16). Anisotropic thermal displacement parameters were assigned for all atoms in all compounds. Crystal structure drawings were produced by SCHAKAL (17) graphics. Detailed crystal data, structure solution, and refinement parameters are given in Tables 1–5, together with the minimum transmission factor for the absorption correction, the extinction, and the absolute structure parameter.

TABLE 1
Crystal Data, Data Collection, and Refinement Parameters for BaTe₂ (I)

Formula	BaTe ₂
Formula weight	392.54
Crystal system	Tetragonal
Space group	I4/mcm (No. 140)
<i>a</i> (Å)	7.181(1)
<i>c</i> (Å)	8.898(2)
Volume (Å ³)	458.8(1)
<i>Z</i>	4
<i>d</i> (calc) (g/cm ³)	5.682
μ (mm ⁻¹)	20.896
Crystal size (mm ³)	0.320 × 0.096 × 0.048
Index range	–9/9, –9/9, 0/11
Reflections collected	913
Independent reflections	152 [<i>R</i> (int) = 0.0278]
Min. transmission factor	0.37
Extinction coefficient	0.0065(4)
Data/restraints/parameters	152/0/8
Final <i>R</i> indices [<i>F</i> _o > 4 σ (<i>F</i> _o)]	<i>R</i> 1 ^a = 1.55%, <i>wR</i> 2 ^a = 3.46%
Final <i>R</i> indices (all data)	<i>R</i> 1 = 1.55%, <i>wR</i> 2 = 3.46%
Goodness-of-fit (GooF)	1.325 ^b
Weighting scheme (<i>A</i> , <i>B</i>) ^c	0.0164, 1.4928
Largest diff. peak and hole (eÅ ⁻³)	0.868, –0.770

^a *R*1 = $\sum (|F_o| - |F_c|) / \sum (|F_o|)$, *wR*2 = $[\sum w(F_o^2 - F_c^2)^2 / \sum wF_o^4]^{1/2}$.

^b GooF = $[\sum w(F_o^2 - F_c^2)^2 / (n - p)]^{1/2}$, where *n* is the number of reflections and *p* is the number of refined parameters.

^c *w* = $1/[\sigma^2 F_o^2 + (AP)^2 + BP]$, where *P* = $(F_o^2 - 2F_c^2)/3$.

TABLE 2
Crystal Data, Data Collection, and Refinement Parameters for
RbTaCu₂Te₄ (II)

Formula	RbTaCu ₂ Te ₄
Formula weight	903.90
Crystal system	Orthorhombic
Space group	<i>P</i> 2 ₁ <i>cn</i> (No. 33)
<i>a</i> (Å)	5.982(2)
<i>b</i> (Å)	20.316(3)
<i>c</i> (Å)	8.192(2)
Volume (Å ³)	995.6(4)
<i>Z</i>	4
<i>d</i> (calc) (g/cm ³)	6.031
μ (mm ⁻¹)	31.459
Crystal size (mm ³)	0.192 × 0.025 × 0.025
Index range	0/7, 0/25, 0/10
Reflections collected	1189
Independent reflections	1189
Min. transmission factor	0.866
Absolute structure parameter	0.001(14)
Data/restraints/parameters	1188/0/72
Final <i>R</i> indices [<i>F</i> _o > 4σ(<i>F</i> _o)]	<i>R</i> 1 ^a = 2.01%, <i>wR</i> 2 ^a = 4.08%
Final <i>R</i> indices (all data)	<i>R</i> 1 = 7.13%, <i>wR</i> 2 = 4.95%
Goodness-of-fit (GooF)	1.084 ^b
Weighting scheme (<i>A</i> , <i>B</i>) ^c	0.0206, 0,0
Largest diff. peak and hole (eÅ ⁻³)	0.947, -1.540

^{a,b,c} See Table 1.

ters (when applied). Atomic coordinates and equivalent isotropic displacement coefficients are listed in Tables 6–10. Supplementary materials include complete crystal

TABLE 3
Crystal Data, Data Collection, and Refinement Parameters for
TaCu₃Te₄ (III)

Formula	TaCu ₃ Te ₄
Formula weight	881.97
Crystal system	Cubic
Space group	<i>P</i> -43 <i>m</i> (No. 215)
<i>a</i> (Å)	5.930(2)
Volume (Å ³)	208.5(1)
<i>Z</i>	1
<i>d</i> (calc) (g/cm ³)	7.023
μ (mm ⁻¹)	34.230
Crystal size (mm ³)	0.03 × 0.03 × 0.03
Index range	-7/7, 0/7, 0/7
Reflections collected	544
Independent reflections	114 [<i>R</i> (int) = 0.0341]
Min. transmission factor	0.511
Absolute structure parameter	0.48(6)
Extinction coefficient	0.010(2)
Data/restraints/parameters	114/0/8
Final <i>R</i> indices (<i>F</i> _o > 4σ(<i>F</i> _o))	<i>R</i> 1 ^a = 2.40%, <i>wR</i> 2 ^a = 6.48%
Final <i>R</i> indices (all data)	<i>R</i> 1 = 2.40%, <i>wR</i> 2 = 6.48%
Goodness-of-fit (GooF)	1.248 ^b
Weighting scheme (<i>A</i> , <i>B</i>) ^c	0.0416, 1.2177
Largest diff. peak and hole (eÅ ⁻³)	1.998, -1.749

^{a,b,c} See Table 1.

TABLE 4
Crystal Data, Data Collection, and Refinement Parameters for
K₂BaSnTe₄ (IV)

Formula	K ₂ BaSnTe ₄
Formula weight	844.63
Crystal system	Cubic
Space group	<i>I</i> -43 <i>m</i> (No. 217)
<i>a</i> (Å)	8.393(1)
Volume (Å ³)	591.2(1)
<i>Z</i>	2
<i>d</i> (calc) (g/cm ³)	4.745
μ (mm ⁻¹)	15.730
Crystal size (mm ³)	0.25 × 0.25 × 0.20
Index range	0/10, 0/10, 0/10
Reflections collected	393
Independent reflections	86 [<i>R</i> (int) = 0.0544]
Min. transmission factor	0.514
Absolute structure parameter	-0.7(6)
Extinction coefficient	0.012(1)
Data/restraints/parameters	86/2/10
Final <i>R</i> indices (<i>F</i> _o > 4σ(<i>F</i> _o))	<i>R</i> 1 ^a = 1.77%, <i>wR</i> 2 ^a = 3.54%
Final <i>R</i> indices (all data)	<i>R</i> 1 = 2.52%, <i>wR</i> 2 = 3.56%
Goodness-of-fit (GooF)	1.349 ^b
Weighting scheme (<i>A</i> , <i>B</i>) ^c	0.0, 3.377
Largest diff. peak and hole (eÅ ⁻³)	1.014, -1.614

^{a,b,c} See Table 1.

data, full list of bond lengths and angles, anisotropic thermal parameters, and tables of *F*_o/*F*_c for all five compounds.

TABLE 5
Crystal Data, Data Collection, and Refinement Parameters for
K₂Ag₂SnTe₄ (V)

Formula	K ₂ Ag ₂ SnTe ₄
Formula weight	923.03
Crystal system	Tetragonal
Space group	<i>I</i> -42 <i>m</i> (No. 121)
<i>a</i> (Å)	8.732(5)
<i>c</i> (Å)	7.425(3)
Volume (Å ³)	566.1(5)
<i>Z</i>	2
<i>d</i> (calc) (g/cm ³)	5.415
μ (mm ⁻¹)	16.381
Crystal size (mm ³)	0.2 × 0.05 × 0.05
Index range	-11/11, 0/11, 0/9
Reflections collected	713
Independent reflections	345 [<i>R</i> (int) = 0.0261]
Min. transmission factor	0.69
Absolute structure parameter	0.0(3)
Data/restraints/parameters	345/1/22
Final <i>R</i> indices (<i>F</i> _o > 4σ(<i>F</i> _o))	<i>R</i> 1 ^a = 3.03%, <i>wR</i> 2 ^a = 7.23%
Final <i>R</i> indices (all data)	<i>R</i> 1 = 3.06%, <i>wR</i> 2 = 7.25%
Goodness-of-fit (GooF)	1.150 ^b
Weighting scheme (<i>A</i> , <i>B</i>) ^c	0.0279, 14.8467
Largest diff. peak and hole (eÅ ⁻³)	1.317, -0.860

^{a,b,c} See Table 1.

TABLE 6
Atomic Coordinates and Equivalent Isotropic Displacement
Parameters (\AA^2) for BaTe_2 (I)

Atom	Site	x	y	z	$U(\text{eq})^a$
Ba	4a	0.0000	0.0000	0.2500	0.0147(2)
Te	8h	0.13649(4)	0.63649(4)	0.0000	0.0161(2)

^a $U(\text{eq})$ is defined as one-third of the trace of the orthogonalized U_{ij} tensor.

TABLE 7
Atomic Coordinates and Equivalent Isotropic Displacement
Parameters (\AA^2) for $\text{RbTaCu}_2\text{Te}_4$ (II)

Atom	Site	x	y	z	$U(\text{eq})^a$
Rb	4a	0.2430(9)	0.56350(7)	0.7565(4)	0.0436(4)
Ta	4a	0.4998(7)	0.35501(2)	0.7443(1)	0.0135(1)
Cu(1)	4a	0.4880(9)	0.2507(2)	-0.0035(3)	0.0219(3)
Cu(2)	4a	0.0000	0.35508(7)	0.7451(4)	0.0228(3)
Te(1)	4a	0.7580(9)	0.24912(3)	0.7463(2)	0.0157(2)
Te(2)	4a	0.7482(9)	0.46003(4)	0.7412(2)	0.0333(2)
Te(3)	4a	0.247(1)	0.35762(9)	0.0060(1)	0.0200(4)
Te(4)	4a	0.248(1)	0.35540(9)	0.4835(1)	0.0211(4)

^a See Table 6.

TABLE 8
Atomic Coordinates and Equivalent Isotropic Displacement
Parameters (\AA^2) for TaCu_3Te_4 (III)

Atom	Site	x	y	z	$U(\text{eq})^a$
Ta	1a	0.0000	0.0000	0.0000	0.0049(5)
Cu	3d	0.5000	0.0000	0.0000	0.0141(7)
Te	4e	0.2580(1)	0.2580(1)	0.2580(1)	0.0089(4)

^a See Table 6.

TABLE 9
Atomic Coordinates and Equivalent Isotropic Displacement
Parameters (\AA^2) for $\text{K}_2\text{BaSnTe}_4$ (IV)

Atom	Site	x	y	z	$U(\text{eq})^a$
K	6b	0.5000	0.0000	0.0000	0.0517(7)
Ba	6b ^b	0.5000	0.0000	0.0000	0.0517(7)
Sn	2a ^b	0.0000	0.0000	0.0000	0.0228(5)
Te	8c	0.31014(6)	0.31014(6)	0.31014(6)	0.0341(4)

^a See Table 6.

^b sof for Ba 0.0416(1); K 0.0834(2).

TABLE 10
Atomic Coordinates and Equivalent Isotropic Displacement
Parameters (\AA^2) for $\text{K}_2\text{Ag}_2\text{SnTe}_4$ (V)

Atom	Site	x	y	z	$U(\text{eq})^a$
K	4c	0.5000	0.0000	0.0000	0.061(2)
Ag(1)	8i ^b	0.1217(3)	0.1217(3)	0.5802(5)	0.063(1)
Ag(2)	2b ^b	0.0000	0.0000	0.5000	0.082(8)
Sn	2a	0.0000	0.0000	0.0000	0.0235(4)
Te	8i	0.32561(7)	0.32561(7)	0.7293(1)	0.0298(3)

^a See Table 6.

^b sof for Ag(1) 0.227(1); Ag(2) 0.023(1).

RESULTS AND DISCUSSION

All five compounds described above were prepared at intermediate temperatures (400–550°C). The structures of these compounds, however, are strikingly different: they range from ‘‘molecular’’ species (zero-dimensional) to layered (two-dimensional) and extended (three-dimensional) networks.

BaTe₂ (I). The Zintl-type compound BaTe_2 has a very simple structure (3h). It contains dimeric $(\text{Te}_2)^{2-}$ units (dumbbells) that stack in a staggered fashion to form infinite pillars along the crystallographic *c*-axis. The 2.772 Å interatomic distance between the two tellurium within a dimeric unit characterizes a typical Te–Te single bond. There are no bonds between the neighboring dimers ($\text{Te} \cdots \text{Te} = 3.94 \text{ \AA}$). The counterion Ba^{2+} rows, also parallel to the *c*-axis, lie between the rows of $(\text{Te}_2)^{2-}$ dumbbells. Figure 1 shows a perspective view of the structure.

BaTe_2 is the second alkaline-earth metal ditelluride synthesized to date. The only other known phase in this

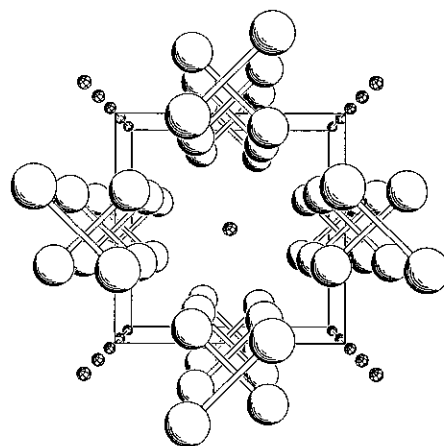


FIG. 1. Projection of the BaTe_2 structure viewed along the *c*-axis. Large partially shaded circles are Te and small cross-hatched circles are Ba. The unit cell is outlined.

family is the cubic MgTe_2 (18) with pyrite structure. Crystals of other known alkaline-earth dichalcogenides were prepared at higher temperatures. For example, high-temperature and high-pressure conditions (900°C , 20 Kbar) were required to crystallize SrS_2 (19a). Single crystals of BaS_2 were obtained by reaction of BaS and S at 800°C (19b). Direct synthesis of the monoclinic BaSe_2 from the elements at $500\text{--}700^\circ\text{C}$ (20) resulted in crystal of poor quality and a rather high R factor (13%).

Among the five known alkaline-earth dichalcogenides, only SrS_2 and BaTe_2 are isostructural. Both barium disulfide (BaS_2) and barium diselenide (BaSe_2) belong to the monoclinic crystal system ($C2/c$, No. 15) with arrays of dichalcogenides $(Q_2)^{2-}$ stacking in an eclipsed manner and with individual rows iso-orientated, whereas BaTe_2 belongs to a tetragonal lattice ($I4/mcm$, No. 140) with the $(\text{Te}_2)^{2-}$ dumbbells stacking in a staggered conformation. MgTe_2 has a different structure from both BaS_2 and BaTe_2 . It belongs to a pyrite-type structure (cubic $Pa-3$, No. 205) with rows of $(\text{Te}_2)^{2-}$ dumbbells stacked in an eclipsed conformation alternating with Mg^{2+} cations. The stacks of $(\text{Te}_2)^{2-}$ dumbbells in this case pack in a herringbone fashion. The common feature of the five AEQ_2 compounds (AE = alkaline-earth metal) is that they all contain a dimeric unit, $(Q_2)^{2-}$. The S–S, Se–Se, and Te–Te distances in SrS_2 , BaS_2 , BaSe_2 , and MgTe_2 are 2.103(5), 2.118, 2.35, and 2.70(1) Å, respectively. The Te–Te separation in BaTe_2 , 2.772 Å, is slightly longer than that in MgTe_2 , and is in good agreement with the Te–Te covalent bond length of 2.74 Å (21).

The alkali metals have a strong ability to form a variety of polychalcogenides with the chalcogen elements. These binary polychalcogenide compounds are chemically very interesting. One important application is their use as precursors in the molten-salt synthesis. The alkaline-earth metals have a much lesser tendency to form polychalcogenides. Only one ditelluride and three tritellurides were previously reported and they are MgTe_2 , BaTe_3 (22), $\text{Ba(en)}_3\text{Te}_3$, $\text{Ba(en)}_{4,5}\text{Te}_3$ (23). The formation of BaTe_2 in the alkali-metal melt suggests the molten-salt technique as an alternative route for the synthesis of alkaline-earth metal ditellurides, tritellurides, or possibly polychalcogenides with even longer oligomeric units.

$\text{RbTaCu}_2\text{Te}_4$ (II). As shown in Fig. 2, $\text{RbTaCu}_2\text{Te}_4$ is a two-dimensional solid consisting of $\text{TaCu}_2\text{Te}_4^-$ layers separated by the Rb^+ ions. The layers run parallel to the (010) plane. The shortest interlayer contact, 4.236(3) Å, is found between Te(2) and Te(3) of the adjacent layers. Therefore, there are virtually no interlayer interactions in this compound. The structure is closely related to $\text{KMgCu}_2\text{Se}_4$ ($M = \text{Nb, Ta}$) which were synthesized at much higher temperatures ($850\text{--}875^\circ\text{C}$) (24a–24c). The atomic coordinations in the two structures are nearly identical, although (II) crystallizes in a different space

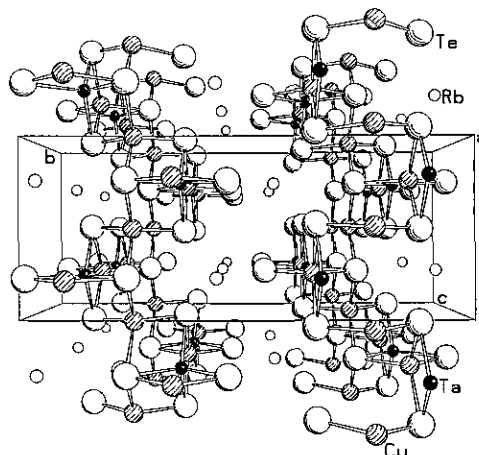


FIG. 2. Perspective view of $\text{RbTaCu}_2\text{Te}_4$ along [100]. Small solid circles are Ta, shaded circles are Cu, large partially shaded circles are Te, and small open circles are Rb. Two $\text{TaCu}_2\text{Te}_4^-$ layers are shown in the figure. The shortest interlayer contact (between Te(1) and Te(2)) is 4.236(3) Å.

group (24d). Both Ta and Cu are tetrahedrally coordinated to the Te in (II). There are four distinct Ta–Te bonds and four distinct Cu(2)–Te bonds, whereas two of the four Cu(1)–Te bonds are identical. Similar bond lengths are observed for all Ta–Te and Cu–Te bonds (2.593–2.648 Å). The interatomic distances between Ta and Cu range from 2.956 to 2.992 Å, significantly longer than the sum of their atomic radii (1/2 of the bond distance) in the Ta and Cu metal (2.70 Å) (25). The edge-sharing TaTe_4 and Cu(2)Te_4 tetrahedra alternate along the a -axis. These parallel, edge-sharing tetrahedral chains are interconnected by corner- and edge-sharing Cu(1)Te_4 tetrahedra. More precisely, the edge-sharing Cu(1)Te_4 and TaTe_4 tetrahedra extend alternately along the c -axis. Cu(1)Te_4 also corner-shares with Cu(2)Te_4 in a similar fashion along both a - and c -axes. Selected bond distances in this compound are listed in Table 11.

The formal oxidation states of the participating atoms may be assigned as the following: $\text{Rb}(+I)$, $\text{Cu}(+I)$, and $\text{Te}(-II)$. This leaves a $+V$ for Ta. Fully oxidized tanta-

TABLE 11
Selected Interatomic Distances (Å) for $\text{RbTaCu}_2\text{Te}_4$ (II)

Ta–Te(1)	2.648(1)	Cu(1)–Te(1)	2.607(3)
Ta–Te(2)	2.600(1)	Cu(1)–Te(1)	2.610(3)
Ta–Te(3)	2.623(3)	Cu(1)–Te(3)	2.607(5)
Ta–Te(4)	2.615(3)	Cu(1)–Te(4)	2.593(5)
Cu(2)–Te(1)	2.594(3)	Ta–Cu(1)	2.956(4)
Cu(2)–Te(2)	2.611(3)	Ta–Cu(1)	2.961(4)
Cu(2)–Te(3)	2.600(4)	Ta–Cu(2)	2.990(4)
Cu(2)–Te(4)	2.605(4)	Ta–Cu(2)	2.992(4)

lum and niobium, or more precisely, tantalum and niobium with formal +5 charge, have been found in a number of solid state sulfide and selenide compounds. Among these are Tl_3MQ_4 ($M = Nb, Ta; Q = S, Se$) (26a), MCu_3Q_4 ($M = Ng, Ta; Q = S, Se$) (24b, 26b), Ta_2PdQ_6 ($Q = S, Se$) (27a), $M_2Pd_3Se_8$ ($M = Nb, Ta$) (27b, 27c), $Ta_2Ni_3S_8$, $Ta_2Pt_3Se_8$ (27d), Cs_3MSe_4 ($M = Nb, Ta$) (27e) and K_3MQ_4 ($M = Nb, Ta; Q = S, Se$) (27f), prepared by direct synthesis or high-temperature crystal growth techniques; $KMCu_2Se_4$ ($M = Nb, Ta$), K_2MCuSe_4 , $K_3Nb_2CuSe_{12}$, and $K_3M_2Cu_3Q_8$ ($M = Nb, Ta; Q = S, Se$) are synthesized from the molten-salt reactions (24). Nb(+V) or Ta(+V) are rarely found in the telluride compounds. The only known example, as far as we are aware, is $NbCu_3Te_4$ (26b). It is interesting to note that the group 5 elements (Nb, Ta) in these structures are usually *tetrahedrally* or *trigonal prismatically* coordinated. Different coordinations of these elements, with lower oxidation states, are often observed in compounds synthesized at high temperatures. Some telluride examples include $MM'Te_2$ ($M = Nb, Ta; M' = Fe, Co, Ni$), $M_4M'Te_4$ ($M = Nb, Ta; M' = Si, Cr, Fe, Co$), $MFe_{1+x}Te_3$ ($M = Ta, Nb; x = 1.25, 1.28$, respectively), TaM'_2Te_2 ($M' = Co, Ni$), $Ta_2M'_3Te_5$ ($M' = Ni, Pd$), and $M_3M'Te_6$ ($M = Nb, Ta; M' = Si, Ge$) in which niobium and tantalum have (distorted) *octahedral* coordination with the tellurium (1, 3, 4a, 4e, 5). Partially oxidized Ta or Nb having coordinations other than octahedral geometry can be found in $Ta_3Pd_3Te_{14}$ (2c) and $[Co_{1.5}Pt_{0.5}]Ta_6PtSe_{16}$ (28). The origin for such a correlation is not yet understood, but we hope that continuing studies of this class of compounds will eventually provide a satisfactory explanation.

Electronic band calculations (29) on a three-dimensional model suggest that $RbTaCu_2Te_4$ is semiconducting (or insulating). The valence band is mainly composed of the Cu 3d and Te 5p orbitals, whereas the Ta 5d states dominate the conduction band (30). The strongest bonding interactions are found between the Ta and the Te atoms. A crystal orbital overlap population (COOP) calculation generated a value of 0.842 for this bond (31). The bonding strength between the two Cu (Cu(1) and Cu(2)) and Te atoms is quite similar. This is reflected by their overlap population values (0.273 and 0.274, respectively). The Cu–Te bonds are significantly weaker than the Ta–Te bonds. The interactions between Ta and two Cu are similar and weakly bonding. The calculated overlap populations are 0.082 for Ta–Cu(1) and 0.074 for Ta–Cu(2), respectively. Our calculations also indicate that addition or removal of several valence electrons in this system (corresponding to an oxidation or reduction process) would have very little effect on Cu–Te and Ta–Cu bonds, but would diminish the Ta–Te bonds significantly.

$TaCu_3Te_4$ (III). This compound is another example in which a formal +V oxidation state of Ta is calculated if

the Cu and Te are assigned Cu^+ and Te^{2-} , respectively. It is a sylvanite type structure (32a, 32b) having a three-dimensional network and it is also isostructural to $NbCu_3Se_4$ (24b) and $MCu_3S_xSe_{4-x}$ ($M = Nb, Ta$) (32c). The structure consists of edge- and corner-sharing tetrahedra of $TaTe_4$ and $CuTe_4$. The three-dimensional nature of (III) is clearly demonstrated in Fig. 3. Note the open channels (cross section $\sim 4.1 \times 4.1 \text{ \AA}$) running parallel to all three axes. The $TaTe_4$ tetrahedra are situated at the eight corners of the cell, and the $CuTe_4$ tetrahedra are located at the middle of the 12 cell edges. Each $TaTe_4$ tetrahedron edge-shares with six $CuTe_4$ tetrahedra along the cell edges, whereas each $CuTe_4$ edge-shares with two $TaTe_4$. The $CuTe_4$ tetrahedra also corner-share with each other along all directions to form a three-dimensional network. The $TaTe_4$ tetrahedron is regular with the angle $Te-Ta-Te = 109.5^\circ$, while $CuTe_4$ is somewhat distorted, with $Te-Cu-Te = 107.8$ and 112.9° . Again, single Ta–Te and Cu–Te bonds are observed in this structure, 2.650(1) and 2.596(1) \AA , respectively. The interatomic distance between Ta and Cu is 2.965(1) \AA , similar to those found in $RbTaCu_2Te_4$.

Three-dimensional band structure of (III) based on the experimental geometry suggests the semiconducting/insulating behavior of $TaCu_3Te_4$ (33). The bonding pattern is very similar to that in (II): the valence band is again mainly Cu 3d and Te 5p states, and the conduction band, mostly Ta 5d states. COOP calculations show that the strongest bonds are between Ta and Te, with an overlap population value of 0.7607. The Cu–Te bonds are considerably weaker, indicated by an overlap population value of 0.2773. The interactions between Cu and Ta are again weakly bonding. An overlap population of 0.0826 is computed for this pair. As in the $RbTaCu_2Te_4$ structure, the

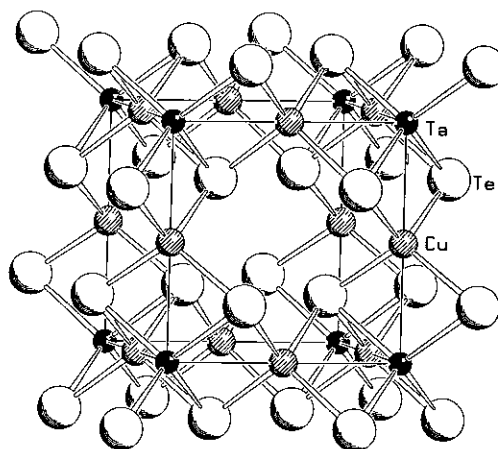


FIG. 3. Projection of $TaCu_3Te_4$. The cubic unit cell is outlined in the figure. Solid circles are Ta, shaded circles are Cu, and large partially shaded circles are Te. The open channels run parallel to all three axes and they have a cross-section of approximately 4.1 by 4.1 \AA .

Ta–Te bonding reaches its maximum in TaCu_3Te_4 . Varying the valence electrons would weaken this bond but have little effect on the Cu–Te and Ta–Cu bonds.

$\text{K}_2\text{BaSnTe}_4$ (IV). Like BaTe_2 , $\text{K}_2\text{BaSnTe}_4$ is also a simple Zintl-type structure isostructural to Tl_3BX_4 ($B = \text{V, Nb}$; $X = \text{S, Se}$) (26a). The formal oxidation state of each atom may be readily assigned: K(+I), Ba(+II), Sn(+IV), and Te(–II). This compound is electron precise and is predicted to be a semiconductor (or insulator). The structure contains isolated SnTe_4^{4-} Zintl anions, located at the eight corners and the center of each cubic unit cell (see Fig. 4). Each Sn atom is surrounded by four tellurium which form a perfect tetrahedral polyhedron. Thus, the structure contains a single short Sn–Te bond, 2.760(1) Å, which is somewhat shorter than the sum of atomic radii of the two atoms, 2.85 Å, and much shorter than the interatomic distance in SnTe, 3.14 Å (25). No short bonding contacts between the tellurium atoms are found, so they exist solely as monotelluride anions, Te^{2-} . The Zintl ions SnQ_4^{4-} ($Q = \text{S, Se, Te}$) are known as stable anions. They have been found in a number of compounds such as the alkali-metal and alkaline-earth metal salts Na_4SnS_4 , Ba_2SnS_4 , and Na_4SnTe_4 (34a–34c). The high coordination ability of SnS_4^{4-} and SnSe_4^{4-} toward transition metal ions has led to a number of extended sulfide and selenide structures, in which they are present as the basic building blocks (34d–34k). Only a few extended telluride structures have been synthesized. One example is the $\text{K}_2\text{HgSnTe}_4$ (1D chain) structure that was recently reported (35). The second one, $\text{K}_2\text{Ag}_2\text{SnTe}_4$ (3D network), was synthesized in our laboratory and will be discussed next.

$\text{K}_2\text{Ag}_2\text{SnTe}_4$ (V). The SnTe_4^{4-} tetrahedron forms the basic construction unit in this structure. They are located at the center and at the corners of the unit cell. They then

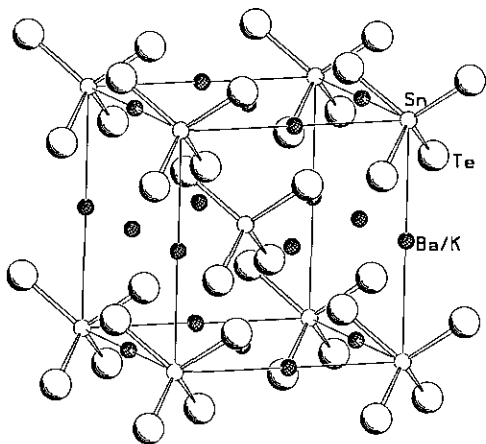


FIG. 4. The structure of $\text{K}_2\text{BaSnTe}_4$. Small open circles are Sn, cross-hatched circles are K/Ba, and large partially shaded circles are Te. The unit cell is outlined.

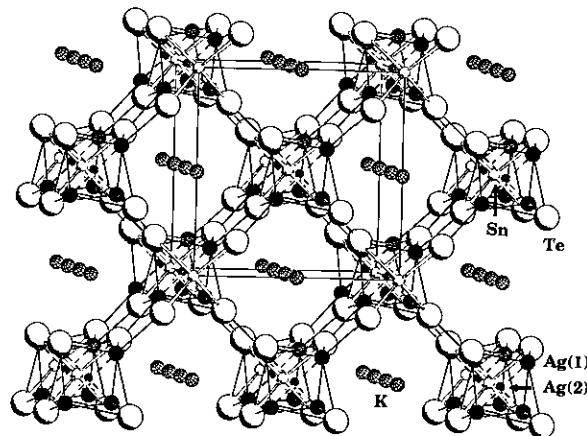


FIG. 5. Projections of the three-dimensional network of $\text{K}_2\text{Ag}_2\text{SnTe}_4$. Small open circles are Sn, medium solid circles are Ag(1), small solid circles are Ag(2), large open circles are Te, and medium cross-hatched circles are K. Large open tunnels with a cross-section approximately 7.2×7.2 Å are parallel to the c -axis.

coordinate to the transition metal atom, Ag, to make a three-dimensional extended network. This 3D network contains large open channels running parallel to the a -axis (cross-section: 7.2×7.2 Å). In the center of the channels are the counterions, K^+ (see Fig. 5). There are two crystallographically distinct silver, Ag(1) and Ag(2). The refinement resulted in partial occupancies for both atoms, $0.454 * 8\text{Ag}(1) + 0.184 * 2\text{Ag}(2) = 4\text{Ag}$ in the unit cell. The Ag(1) atom has a (distorted) tetrahedral coordination with Te. There are three distinct Ag(1)–Te bonds, 2.686(4), 2.750(4), and $2 \times 2.983(3)$ Å, but a single Ag(2)–Te bond, 2.946(1) Å, and a single Sn–Te bond, 2.745(1) Å. The Ag(1) atoms also form Ag_4 tetrahedra around the Ag(2) site. If fully occupied, there would be six extremely short Ag–Ag contacts within each tetrahedron [Ag(1)–Ag(1): $2 \times 2.437(6)$ Å, Ag(1)–Ag(2): $4 \times 1.617(4)$ Å]. Since the site occupancies give 1.82 Ag(1) atoms and 0.184 Ag(2) per tetrahedron, presumably there can only be one pair of Ag(1) atoms or a single Ag(2) at any given time. The Ag(1)–Ag(1) distance between this pair is most likely the longest one in the tetrahedron, 3.006(7) Å. Further study to rationalize the disorder is in progress.

No short Te–Te contact is detected in (V) and an unambiguous oxidation state can be assigned to each atom in this structure: K(I), Ag(I), Sn(IV), and Te(–II). To our understanding, (V) is the first example of solid state transition metal telluride containing a three-dimensional network that is stabilized by the SnTe_4^{4-} ion. Other extended telluride structures assembled from tetrahedral $M\text{Te}_4$ building blocks include one-dimensional Rb_2SnTe_5 (36) and three-dimensional $\text{CaGa}_6\text{Te}_{10}$ and $\text{CaAl}_6\text{Te}_{10}$ (37). The discovery of the $\text{K}_2\text{Ag}_2\text{SnTe}_4$ structure has certainly demonstrated the potential of finding other extended transition metal telluride phases.

CONCLUSIONS

Several new binary, ternary, and quaternary metal tellurides have been successfully synthesized at intermediate temperatures employing low-melting alkali-metal polytellurides as fluxes (solvents). The crystal structures of these compounds have been determined by single crystal X-ray diffraction methods. The structures range from molecular to extended two- and three-dimensional solids. Except for the ditelluride BaTe_2 , which contains short Te-Te bonds (2.772 Å), all other four structures are monotellurides. Interesting correlations between the coordination geometry and the oxidation state of Ta in $\text{RbTaCu}_2\text{Te}_4$ and TaCu_3Te_4 have been revealed. Extended Hückel band calculations show similar bonding patterns in these two structures. $\text{K}_2\text{Ag}_2\text{SnTe}_4$ is the first example of extended transition-metal tellurides constructed from the SnTe_4^- building unit.

ACKNOWLEDGMENTS

Financial support from Research Corporation through its Schering-Plough Award and Bristol-Myers Squibb Company Award is greatly acknowledged. We are grateful to the Petroleum Research Fund, administered by the American Chemical Society. J.L. and H.Y.G. thank professor M. G. Kanatzidis for many helpful discussions. This work has made use of the microprobe and X-ray facilities at Rutgers University and the University of Milan, Italy. We also thank Reviewer II for his insightful comments.

REFERENCES

- (a) B.-Q. Huang, M. Shang, and J.-L. Huang, *Jiegou Huaxue (J. Struct. Chem.)* **7**, 133 (1988); (b) B.-Q. Huang, J.-L. Huang, and S.-X. Liu, *Jiegou Huaxue (J. Struct. Chem.)* **8**, 145 (1989); (c) J.-L. Huang, S.-X. Liu, and B.-Q. Huang, *Sci. China Ser. B* **34**, 666 (1991).
- (a) E. W. Liimatta and J. A. Ibers, *J. Solid State Chem.* **71**, 384 (1987); (b) E. W. Liimatta and J. A. Ibers, *J. Solid State Chem.* **77**, 141 (1988); (c) E. W. Liimatta and J. A. Ibers, *J. Solid State Chem.* **78**, 7 (1989); (d) A. Mar and J. A. Ibers, *J. Solid State Chem.* **92**, 352 (1991); (e) A. Mar and J. A. Ibers, *J. Chem. Soc. Dalton Trans.*, 639 (1991); (f) P. M. Keane and J. A. Ibers, *Inorg. Chem.* **30**, 1327 (1991); (g) P. M. Keane and J. A. Ibers, *Inorg. Chem.* **30**, 3096 (1991); (h) P. M. Keane and J. A. Ibers, *J. Solid State Chem.* **93**, 291 (1991); (i) A. Mar and J. A. Ibers, *J. Solid State Chem.* **97**, 366 (1992); (j) A. Mar and J. A. Ibers, *J. Am. Chem. Soc.* **115**, 3227 (1993); (k) J. A. Cody and J. A. Ibers, *Inorg. Chem.* **33**, 2713 (1994).
- (a) J. Li, M. E. Badding, and F. J. DiSalvo, *Inorg. Chem.* **31**, 1050 (1992); (b) J. Li, M. E. Badding, and F. J. DiSalvo, *J. Less-Common Met.* **184**, 257 (1992); (c) J. Li and P. Carroll, *Mater. Res. Bull.* **27**, 1073 (1992); (d) M. E. Badding, J. Li, F. J. DiSalvo, W. Zhou, and P. P. Edwards, *J. Solid State Chem.* **100**, 313 (1992); (e) J. Li, S. L. McDonnell, and F. McCulley, *J. Alloys Compounds* **197**, 21 (1993); (f) J. Li, F. McCulley, S. L. McDonnell, N. Masciocchi, D. M. Proserpio, and A. Sironi, *Inorg. Chem.* **32**, 4829 (1993); (g) J. Li, F. McCulley, M. J. Dioszeghy, S. C. Chen, K. V. Ramanujachary, and M. Greenblatt, *Inorg. Chem.* **33**, 2109 (1994); (h) J. Li, H.-Y. Guo, J. R. Carey, S. Mulley, D. M. Proserpio, and A. Sironi, *Mater. Res. Bull.* **29**, 1041 (1994).
- (a) M. E. Badding and F. J. DiSalvo, *Inorg. Chem.* **29**, 3952 (1990); (b) Y. Park and M. G. Kanatzidis, *Chem. Mater.* **3**, 781 (1991); (c) Y. Park and M. G. Kanatzidis, *Angew. Chem. Int. Ed. Engl.* **30**, 1325 (1991); (d) X. Zhang and M. G. Kanatzidis, *private communications*; (e) L. Monconduit, M. Evain, F. Boucher, R. Brec, and J. Rouxel, *Z. Anorg. Allg. Chem.* **616**, 177 (1992).
- (a) W. Tremel, *J. Chem. Soc. Chem. Commun.*, 1405 (1991); (b) W. Tremel, Habilitationsschrift. Universität Münster, 1991; (c) W. Tremel, *Angew. Chem. Int. Ed. Engl.* **30**, 840 (1991); (d) W. Tremel, *Angew. Chem. Int. Ed. Engl.* **31**, 217 (1992); (e) W. Tremel, *Inorg. Chem.* **31**, 755 (1992).
- (a) J. Li, R. Hoffmann, M. E. Badding, and F. J. DiSalvo, *Inorg. Chem.* **29**, 3943 (1990); (b) J.-F. Halet, R. Hoffmann, W. Tremel, E. W. Liimatta, and J. A. Ibers, *Chem. Mater.* **1**, 451 (1989); (c) E. Canadell, L. Monconduit, R. Evain, R. Brec, J. Rouxel, and M.-H. Whangbo, *Inorg. Chem.* **32**, 10 (1993); (d) A. van de Lee, M. Evain, L. Monconduit, and R. Brec, *Inorg. Chem.* **33**, 3032 (1994); (e) K. Ahn, T. Hughbanks, K. D. D. Rathnayaka, and D. G. Naugle, *Chem. Mater.* **6**, 418 (1994); (f) R. Abdon and T. Hughbanks, *Chem. Mater.* **6**, 424 (1994).
- (a) C. J. Warren, D. M. Ho, R. C. Haushalter, and A. B. Bocarsly, *Angew. Chem. Int. Ed. Engl.* **32**, 1646 (1993); (b) C. J. Warren, D. M. Ho, and A. B. Bocarsly, *J. Am. Chem. Soc.* **115**, 6416 (1993); (c) C. J. Warren, S. S. Dhingra, D. M. Ho, R. C. Haushalter, and A. B. Bocarsly, *Inorg. Chem.* **33**, 2709 (1994); (d) C. J. Warren, R. C. Haushalter, and A. B. Bocarsly, *Chem. Mater.* **6**, 780 (1994); (e) S. S. Dhingra and R. C. Haushalter, *Inorg. Chem.* **33**, 2735 (1994).
- (a) H. Schäfer, "Chemical Transport Reactions." Academic Press, New York 1964; (b) F. Rosenberger, in "Preparation and Characterization of Materials" (J. M. Ronig and C. N. R. Rao, Eds.), Oxford Univ. Press, Oxford, 1987.
- (a) H. Bloom, "The Chemistry of Molten Salts," Benjamin, New York, 1967; (b) G. Mamantov, "Molten Salts: Characterization and Analysis. Dekker, New York, 1969; (c) D. Elwell and H. J. Scheel, "Crystal Growth from High-Temperature Solutions." Academic Press, London, 1975.
- S. A. Sunshine and J. A. Ibers, *J. Am. Chem. Soc.* **109**, 6202 (1987).
- M. G. Kanatzidis, *Chem. Mater.* **2**, 353 (1990).
- J.-H. Liao, C. Varotsis, and M. G. Kanatzidis, *Inorg. Chem.* **32**, 2453 (1993).
- A. Altomare, G. Cascarano, C. Giacovazzo, A. Guagliardi, M. C. Burla, G. Polidori, and M. Camalli, "SIR92," *J. Appl. Crystallogr.* **27**, 435 (1994).
- G. M. Sheldrick, "SHELXL-93: Program for Crystal Structure Refinement", University of Goettingen, 1994.
- A. C. T. North, D. C. Phillips, and F. S. Methews, *Acta Crystallogr. Sect. A* **24**, 351 (1968).
- H. D. Flack, *Acta Crystallogr. Sect. A* **41**, 500 (1985).
- E. Keller, "SCHAKAL92, a Computer Program for the Graphical Representation of Crystallographic Models." University of Freiburg, Germany.
- S. Yanagisawa, M. Tashiro, and S. Anzai, *J. Inorg. Nucl. Chem.* **31**, 943 (1969).
- (a) I. Kawada, K. Kato, and S. Yamaoka, *Acta Crystallogr. Sect. B* **32**, 3110 (1976); (b) I. Kawada, K. Kato, and S. Yamaoka, *Acta Crystallogr. Sect. B* **31**, 2905 (1975).
- F. Hulliger and T. Siegrist, *Z. Naturforsch. B* **36**, 14 (1981).
- L. Pauling, "The Nature of the Chemical Bond." Cornell Univ. Press, Ithaca, NY, 1960.
- G. Cordier, C. Schwidetzky, and H. Schäfer, *Z. Naturforsch. B* **39**, 833 (1984).
- R. Zagler, B. Eisenmann, and H. Schäfer, *Z. Naturforsch. B* **42**, 151 (1987).

24. (a) Y.-J. Lu and J. A. Ibers, *J. Solid State Chem.* **94**, 381 (1991); (b) Y.-J. Lu and J. A. Ibers, *J. Solid State Chem.* **107**, 58 (1993); (c) Y.-J. Lu and J. A. Ibers, *J. Solid State Chem.* **111**, 447 (1994); (d) The structure of (II) has been refined in space group $Pna2_1$ with a nonstandard setting $P2_1cn$ to allow better comparison with the coordinates of $\text{KNbCu}_2\text{Se}_4$ previously reported in the space group $C2cm$ (24a). In our case, the choice of a C -centered space group would not explain the weak but observed reflections having $h + k = \text{odd}$; (e) Y.-J. Lu and J. A. Ibers, *Inorg. Chem.* **30**, 3317 (1991); (f) Y.-J. Lu and J. A. Ibers, *J. Solid State Chem.* **98**, 312 (1992).
25. J. C. Slater, "Quantum Theory of Molecules and Solids," Vol. II, p. 236. McGraw-Hill, New York, 1965.
26. (a) C. Crevecoeur, *Acta Crystallogr.* **17**, 757 (1964); (b) H. Hulliger, *Helv. Phys. Acta* **34**, 379 (1961).
27. (a) D. A. Keszler, P. J. Squattrito, N. E. Brese, J. A. Ibers, M. Shang, and J. Lu, *Inorg. Chem.* **24**, 3063 (1985); (b) D. A. Keszler and J. A. Ibers, *J. Solid State Chem.* **52**, 73 (1984); (c) D. A. Keszler, J. A. Ibers, S. Shang, and J. Lu, *J. Solid State Chem.* **57**, 68 (1985); (d) P. J. Squattrito, S. A. Sunshine, and J. A. Ibers, *J. Solid State Chem.* **64**, 261 (1986); (e) H. Yun, C. R. Randall, and J. A. Ibers, *J. Solid State Chem.* **76**, 109 (1988); (f) M. Latroche and J. A. Ibers, *Inorg. Chem.* **29**, 1503 (1990).
28. A. Sunshine and J. A. Ibers, *J. Solid State Chem.* **69**, 219 (1987).
29. (a) R. Hoffmann, *J. Chem. Phys.* **39**, 1397 (1963); (b) R. Hoffmann and W. N. Lipscomb, *J. Chem. Phys.* **36**, 2179 and 3489 (1962); **37**, 2872 (1962); (c) R. Hoffmann and M.-H. Whangbo, *J. Am. Chem. Soc.* **100**, 6093 (1978); (d) R. Hoffmann, "Solids and Surfaces: A Chemist's View of Bonding in Extended Structures." VCH, New York, 1988.
30. The parameters used in the calculations are from Ref. (6a). M.-H. Whangbo and P. Gressier, *Inorg. Chem.* **23**, 1228 (1984); M.-H. Whangbo and E. Canadell, *Inorg. Chem.* **29**, 1395 (1990). A 108 k-point set was used in the average property calculations.
31. See, for example, (a) S. D. Wijeyesekera and R. Hoffmann, *Organometallics* **3**, 949 (1984); (b) M. Kertesz and R. Hoffmann, *J. Am. Chem. Soc.* **106**, 3453 (1984); (c) J.-Y. Saillard and R. Hoffmann, *J. Am. Chem. Soc.* **106**, 2006 (1984).
32. (a) F. J. Trojer, *Am. Mineral.* **51**, 890 (1966); (b) L. Pauling and R. Hultgren, *Z. Kristallogr.* **84**, 204 (1933); (c) A. Muller and W. Sievert, *Z. Anorg. Allg. Chem.* **406**, 80 (1974).
33. The same parameters used in the calculations of $\text{RbTaCu}_2\text{Te}_4$ were taken here.
34. (a) K. Susa and H. Steinfink, *J. Solid State Chem.* **3**, 75 (1971); (b) J.-C. Jumas, E. Philippot, F. Vermot-Gaud-Daniel, M. Ribes, and M. Maurin, *J. Solid State Chem.* **14**, 319 (1975); (c) B. Eisenmann, H. Schäfer, and H. Schrod, *Z. Naturforsch. B* **38**, 7 (1983); (d) Chr. L. Teske, *Z. Anorg. Allg. Chem.* **419**, 67 (1976); (e) Chr. L. Teske and O. Vetter, *Z. Anorg. Allg. Chem.* **426**, 281 (1976); **427**, 200 (1976); (f) Chr. L. Teske, *Z. Anorg. Allg. Chem.* **445**, 193 (1978); (g) Chr. L. Teske, *Z. Anorg. Allg. Chem.* **460**, 163 (1980); (h) Chr. L. Teske, *Z. Naturforsch. B* **35**, 7 (1980); (i) Guen and W. S. Glaunsinger, *J. Solid State Chem.* **35**, 10 (1980); (j) P. Wu, Y.-J. Lu, and J. A. Ibers, *J. Solid State Chem.* **97**, 383 (1992); (k) J.-H. Liao and M. G. Kanatzidis, *Chem. Mater.* **5**, 1561 (1993).
35. S. S. Dhingra and R. C. Haushalter, submitted for publication.
36. C. Brinkmann, B. Eisenmann, and H. Schäfer, *Mater. Res. Bull.* **20**, 299 (1985).
37. W. Klee and H. Schäfer, *Z. Naturforsch. B* **34**, 657 (1979).